

## Stable cerium isotopes as a tracer of oxidation reactions

P. Bonnand, M. Boyet, C. Bosq

### Supplementary Information

The Supplementary Information includes:

- Materials and Methods
- Tables S-1 to S-3
- Supplementary Information References

### Materials and Methods

The silicate samples are international rock standards (BCR-2, W2, GSP-2, BHVO-2 and AGV-2). Their REE concentrations are reported in Table S-1.

Several carbonate samples analysed in this study are international rock standards (JDo-1, Cal-S, BCS CRM 513 and BCS CRM 393). I27 is a Neoproterozoic carbonate sample from Islay (Scotland). B08 is a modern ooids sample from the Bahamas. C171 is an oolitic limestone from the Caswell Bay oolite. Their chemical compositions have been previously investigated (Bonnand *et al.*, 2013). Pt1 and Pt5 are two upper Jurassic carbonates studied by Olivier and Boyet (2006). The REE concentrations and the Ce anomalies ( $Ce/Ce^*$ ) are presented in Tables S-1 and S-2, respectively. The samples are a combination of limestones and dolomite and have been selected to cover a large range of elemental Ce anomalies. The  $Ce/Ce^*$  values are calculated using geometric extrapolation and the equation  $Ce/Ce^* = Ce/(Pr^2/Nd)$  from Lawrence *et al.* (2006).

The BIF samples have been previously investigated for their chemical composition and their radiogenic cerium isotopic composition (Bonnand *et al.*, 2020). The samples are from the 3.22 Ga Moodies Group of the Barberton Greenstone Belt which is comprised of sand- and siltstone, subordinate conglomerate and volcanics, and minor ferruginous sediment that were mostly deposited in shallow-marine and/or terrestrial settings (*e.g.*, Heubeck, 2019). The samples have been selected to cover the large Ce anomaly previously described at this locality.

The Mn nodule samples are two USGS standards (NOD-A1 and NOD-P1). They are believed to be from mixed sources (a combination of hydrogenetic and diagenetic formation). The Ce anomaly measured for the Mn nodules samples are presented in supplementary Table S-1.

### Chemical dissolution procedure for natural samples

The dissolution procedures vary depending on the nature of the samples. For silicate samples, the dissolution was achieved by adding a HF–HNO<sub>3</sub> mixture (3:1 ratio) to the sample powders. The beakers were placed on the hotplate at 90 °C for at least 24 h. The samples were then treated with 6 M HCl to remove the fluorides formed during the dissolution. For the carbonate samples, a weak room temperature acetic acid (0.5 M) dissolution procedure was used in order to avoid the dissolution of detrital components. The BIF and nodule samples were dissolved using a 6 M HCl room temperature dissolution procedure.

### Triple spike

In order to correct for mass fractionation during chemical separation and measurements on the mass spectrometer, a triple spike method was developed and is fully described in Bonnand *et al.* (2019). The Ce isotopic composition is reported as the per mil variation from the Ce isotope standard LMV using the equation:

$$\delta^{142}\text{Ce} = \left( \frac{{}^{142}\text{Ce}/{}^{140}\text{Ce}_{\text{sample}}}{{}^{142}\text{Ce}/{}^{140}\text{Ce}_{\text{LMV}}} - 1 \right) \times 1000. \quad \text{Eq. S-1}$$

The LMV Ce standard has been prepared from AMES metal (Bonnand *et al.*, 2019) and is available on request.

### Chemical separation procedures

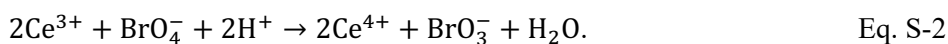
The chemical separation method used in this study is modified after Tazoe *et al.* (2007), Li *et al.* (2015), Bellot *et al.* (2015) and Bonnand *et al.* (2019). The chemical separation developed to separate the Ce fraction from silicate matrices involved three column chemistries. For the first step of the separation procedure, the samples were loaded onto 1 mL of AG50 X8 200–400 mesh resin in 2.5 N HCl. The REE stuck to the resin while the main cations were eluted from the resin. The first step of the procedure was designed to isolate the REEs from the main cations of the matrix. The first chemistry also allowed the separation between REE and Ba (one of the main isobaric interference). During this first chemical separation, Ba was then eluted in 2 M HNO<sub>3</sub> and the REE were eluted in 6 M HCl. The second column procedure was designed to separate Ce<sup>4+</sup> from the other REE (La and Nd) and followed the procedure proposed by Tazoe *et al.* (2007). The chemical separation procedure was tested for blanks



and yield. We obtained yields that were 99.9 % for this chemistry and the blanks were less than 0.2 ng of Ce. The oxidation of  $\text{Ce}^{3+}$  to  $\text{Ce}^{4+}$  was achieved with 0.5 mL of  $\text{NaBrO}_3$  (20 mM) in 10 M  $\text{HNO}_3$ . The samples were loaded in 10 M  $\text{HNO}_3$  +  $\text{NaBrO}_3$  onto 0.2 mL LnSpec Eichrom resin (50–100  $\mu\text{m}$ ). During this step of the chemical procedure,  $\text{Ce}^{4+}$  stuck to the resin while all  $\text{REE}^{3+}$  were eluted in the loading solution. The Ce fraction (present as  $\text{Ce}^{4+}$ ) was eluted in 6 M  $\text{HCl}$  +  $\text{H}_2\text{O}_2$ . Finally, the samples were then processed through the first step of the chemistry (AG50 X8, 200–400 mesh) to make sure the Ce fraction was free of any remaining matrix cations. For the seawater derived samples (carbonates, banded iron formations and Mn nodules), another column was performed prior to the protocol described above. For the carbonate samples, the samples were processed through a TRU spec resin in 1 M  $\text{HNO}_3$ . In this chemistry, Ce sticks to the resin and the Ca from the matrix does not. For the banded iron formation and the Mn nodules, Fe was removed by processing the samples through an anionic column. To this end, the samples were loaded onto AG1 X8 resin in 6 M  $\text{HCl}$ . In these conditions, Fe sticks to the resin and the cerium fraction does not. The total procedural blank was better than 0.4 ng of Ce.

### Oxidation experiments

The oxidation experiments were performed at room temperature in the clean laboratory. The oxidation experiments are based on the chemical separation procedure performed in the step 2 of the protocol described above, but rather than using excess perbromic acid to ensure complete oxidation of  $\text{Ce}^{3+}$  to  $\text{Ce}^{4+}$ , variable concentrations of perbromic acid were employed. The two redox couples involved in this oxidation reaction are  $\text{Ce}^{3+}/\text{Ce}^{4+}$  and  $\text{BrO}_4^-/\text{BrO}_3^-$ . The oxidative capacity of perbromic acid has been described in Appelman (1969). The oxidation reaction can be summarised as:



For the partial oxidation experiments, a  $\text{Ce}^{3+}$  solution was first dried down in a beaker. In order to achieve variable degrees of oxidation, we added different amount of  $\text{NaBrO}_3$  in 10 M  $\text{HNO}_3$  to the samples (from 0.0008 to 0.04 mmol  $\text{NaBrO}_3$ ). Two series of experiments were performed with two durations of oxidation (3 and 20 minutes). The 3 minutes experiments were performed in three different sessions in the laboratory. The two fractions ( $\text{Ce}^{3+}$  and  $\text{Ce}^{4+}$ ) were then isolated by processing the solution through the step 2 of the chemical purification procedure without further treatment. The partially oxidised solutions were directly loaded onto the Ln resin without additional processing. During this chemical procedure, the solutions (with both  $\text{Ce}^{3+}$  and  $\text{Ce}^{4+}$ ) were loaded in 10 M  $\text{HNO}_3$  + variable  $\text{NaBrO}_3$  onto 0.2 mL LnSpec Eichrom resin (50–100  $\mu\text{m}$ ). During this step of the chemical procedure, the fraction of  $\text{Ce}^{3+}$  is directly collected because it is eluted in the loading solution. The  $\text{Ce}^{4+}$  fraction sticks to the resin and is then collected later, once a solution of 6 M  $\text{HCl}$  +  $\text{H}_2\text{O}_2$  is added. After separation, the  $\text{Ce}^{4+}$  fraction was aliquoted and the Ce concentration was measured on the quadrupole ICP-MS



(Agilent 7500). The possibility of Ce loss *via* precipitation of CeO<sub>2</sub>(s) is excluded considering the recently determined solubility constant for nanoparticulate CeO<sub>2</sub>(s) (Plakhova *et al.*, 2016) that supports strong undersaturation in our experimental procedures. The amount of Ce<sup>3+</sup> was thus calculated assuming a 100 % recovery (see above subsection ‘Chemical separation procedure’). The Ce<sup>3+</sup> and Ce<sup>4+</sup> fractions were then spiked with the requisite amount of Triple spike. In order to remove the Na added during the oxidation procedure, the samples were cleaned using a single chromatography procedure using cation resin AG50 X8 (described above as the first step of the chemical procedure for natural samples) and measured on the TIMS Triton Plus, following the procedures described below.

### Mass spectrometry

Isotopic measurements were performed on a ThermoScientific Thermal Ionisation Mass spectrometer Triton Plus (TIMS) at the Laboratoire Magmas et Volcans. The Ce standards and samples were analysed in oxide forms using the double filament technique. The Ce fraction was loaded in HCl onto outgassed Re wire together with 0.5 µL of 1 M H<sub>3</sub>PO<sub>4</sub>. The cup configuration used is described in Bonnand *et al.* (2019) and allows the simultaneous measurements of Ce isotopes (<sup>136</sup>Ce, <sup>138</sup>Ce, <sup>140</sup>Ce and <sup>142</sup>Ce) and half masses necessary for the tailing correction. The Ce masses and the tailing are measured with 10<sup>11</sup> and 10<sup>13</sup> Ω resistors, respectively. Typical runs on the mass spectrometer consist of 27 blocks of 20 cycles with 8.462 seconds integration time. Each block started with a baseline measurement of 30 seconds. The gain calibrations for the 10<sup>11</sup> and 10<sup>13</sup> Ω resistors were performed daily using the ThermoScientific software built in gain routine (at 0.33 V). The Ce isotopic composition of the samples and standards was determined offline but baseline and gain corrections were performed online with the ThermoScientific software. The deconvolution procedure for both unspiked and spiked runs can be divided in three main steps: tail correction on mass <sup>136</sup>Ce and <sup>138</sup>Ce, oxide corrections and mass bias fractionation corrections and is performed offline.

The reproducibility of our mass spectrometry technique has been assessed by multiple measurements of our Ce<sub>LMV</sub> standard without chemical separation ( $\delta^{142}\text{Ce}_{\text{LMV}} = 0.000 \pm 0.037 \text{ ‰}$  (2 s.d.;  $n = 5$ ). The accuracy was assessed with analyses of the Ce<sub>LMV</sub> standard after chemical purification for each sample’s matrices. The data is given in Table S-3. The results obtained with the three separation procedures (silicate, carbonate and Fe-rich) are all within error of the unpurified Ce<sub>LMV</sub> standard solution (see Table S-3). The external reproducibility of our analytical technique has been determined by multiple measurements of two geological reference material. To this end, BHVO-2 and GSP-2 were measured several times and we obtained  $\delta^{142}\text{Ce}$  values of  $0.087 \pm 0.045 \text{ ‰}$  ( $n = 4$ ) and  $0.045 \pm 0.044 \text{ ‰}$  ( $n = 4$ ), respectively. The value obtained for the JDo-1 Dolomite standard is slightly heavier than the published values by Nakada *et al.* (2019). It is however important to note that the normalising standard is different and direct comparison of  $\delta^{142}\text{Ce}$  value is impossible.



## Supplementary Tables

**Table S-1** Ce quantities and Ce isotopic compositions in the oxidation experiments (See text for details of the experimental settings). The 2 s.e. is the internal error of the Ce measurements.

Sample name	Oxidation time (min)	Ce <sup>3+</sup> (ng)	Ce <sup>4+</sup> (ng)	Ce <sup>4+</sup> /Ce <sub>TOT</sub>	δ <sup>142</sup> Ce(III) (‰)	2 s.e.	δ <sup>142</sup> Ce(IV) (‰)	2 s.e.
OE5	3	bdl	3000	1.00	n.d.	n.d.	-0.010	0.004
OE6	3	247	2753	0.92	0.141	0.007	0.006	0.005
OE7	3	700	2300	0.77	0.245	0.006	-0.061	0.009
OE8	3	2100	900	0.30	0.053	0.010	-0.295	0.007
OE9	3	2721	279	0.09	-0.015	0.011	-0.347	0.006
OE10	3	0	3000	1.00	n.d.	n.d.	0.028	0.004
OE11	3	4	2996	1.00	n.d.	n.d.	0.022	0.007
OE12	3	39	2961	0.99	n.d.	n.d.	0.017	0.006
OE13	3	232	2768	0.92	0.223	0.004	-0.061	0.007
OE14	3	832	2168	0.72	0.101	0.004	-0.081	0.008
OE15	3	1046	1954	0.65	0.182	0.007	-0.109	0.014
OE16	3	1485	1515	0.51	0.147	0.010	-0.207	0.009
OE17	3	451	2549	0.85	0.399	0.005	-0.074	0.011
OE18	3	1196	1804	0.60	0.169	0.006	-0.108	0.007
OE19	3	1760	1240	0.41	0.073	0.019	-0.139	0.005
OE20	3	2497	503	0.17	-0.024	0.004	n.d.	n.d.
OE21	3	2696	304	0.10	-0.022	0.004	n.d.	n.d.
OE22	20	bdl	2988	1.00	n.d.	n.d.	0.017	0.006
OE23	20	386	2613	0.87	-0.021	0.004	0.026	0.007
OE24	20	1228	1771	0.59	-0.055	0.006	0.030	0.010
OE25	20	2021	978	0.33	0.042	0.007	-0.059	0.008
OE26	20	2821	178	0.06	0.016	0.007	n.d.	n.d.

bdl, below detection limit; n.d., not determined.

**Table S-2** Ce isotopic compositions and elemental Cerium anomaly (Ce/Ce\*) in the studied samples. The 2 s.e. is the internal error of the Ce measurements.

Sample name	$\delta^{142}\text{Ce}$ (‰)	2 s.e.	Ce/Ce*
AGV2	0.069	0.005	1.01
BCR-2	0.058	0.005	1.04
BHVO-2	0.087	0.004	1.02
W2	0.096	0.007	0.97
GSP2	0.045	0.004	0.99
Jdo-1	0.337	0.005	0.27
Cal-S	0.100	0.012	0.44
BCS CRM 393	0.179	0.005	0.65
BCS CRM 513	0.123	0.005	0.69
C171	0.217	0.007	0.35
Pt1	0.111	0.006	0.58
Pt5	0.081	0.013	0.83
B08	0.186	0.015	0.87
I27	0.119	0.009	1.19
average carbonates	0.161	0.160 <sup>†</sup>	
IK14-3	-0.032	0.004	0.92
IK14-12b	-0.055	0.005	1.12
IK14-18	-0.007	0.005	0.39
14-37	-0.015	0.004	1.17
average BIF	-0.027	0.042 <sup>†</sup>	
NOD-A1	0.116	0.005	4.18
NOD-P1	0.142	0.004	1.53
average nodules	0.129	0.037 <sup>†</sup>	

<sup>†</sup>2 s.d.

**Table S-3** REE concentrations for the analysed samples and Ce isotopic composition for analytical tests.

Table S-3 (.xlsx) is available for download from the online version of this article at <https://doi.org/10.7185/geochemlet.2340>.



## Supplementary Information References

- Appelman, E.H. (1969) Perbromic acid and perbromates: synthesis and some properties. *Inorganic Chemistry* 8, 223–227. <https://doi.org/10.1021/ic50072a008>
- Bellot, N., Boyet, M., Doucelance, R., Pin, C., Chauvel, C., Auclair, D. (2015) Ce isotope systematics of island arc lavas from the Lesser Antilles. *Geochimica et Cosmochimica Acta* 168, 261–279. <https://doi.org/10.1016/j.gca.2015.07.002>
- Bonnand, P., James, R.H., Parkinson, I.J., Connelly, D.P., Fairchild, I.J. (2013) The chromium isotopic composition of seawater and marine carbonates. *Earth and Planetary Science Letters* 382, 10–20. <https://doi.org/10.1016/j.epsl.2013.09.001>
- Bonnand, P., Israel, C., Boyet, M., Doucelance, R., Auclair, D. (2019) Radiogenic and stable Ce isotope measurements by thermal ionisation mass spectrometry. *Journal of Analytical Atomic Spectrometry* 34, 504–516. <https://doi.org/10.1039/C8JA00362A>
- Bonnand, P., Lalonde, S.V., Boyet, M., Heubeck, C., Homann, M., Nonnotte, P., Foster, I., Konhauser, K.O., Köhler, I. (2020) Post-depositional REE mobility in a Paleoarchean banded iron formation revealed by La-Ce geochronology: A cautionary tale for signals of ancient oxygenation. *Earth and Planetary Science Letters* 547, 116452. <https://doi.org/10.1016/j.epsl.2020.116452>
- Heubeck, C. (2019) The Moodies Group—a High-Resolution Archive of Archaean Surface Processes and Basin-Forming Mechanisms. In: Kröner, A., Hofmann, A. (Eds.) *The Archaean Geology of the Kaapvaal Craton, Southern Africa*. Regional Geology Reviews. Springer, Cham., 133–169. [https://doi.org/10.1007/978-3-319-78652-0\\_6](https://doi.org/10.1007/978-3-319-78652-0_6)
- Lawrence, M.G., Jupiter, S.D., Kamber, B.S. (2006) Aquatic geochemistry of the rare earth elements and yttrium in the Pioneer River catchment, Australia. *Marine and Freshwater Research* 57, 725–736. <https://doi.org/10.1071/MF05229>
- Li, C.-F., Wang, X.-C., Li, Y.-L., Chu, Z.-Y., Guo, J.-H., Li, X.-H. (2015) Ce-Nd separation by solid-phase micro-extraction and its application to high-precision  $^{142}\text{Nd}/^{144}\text{Nd}$  measurements using TIMS in geological materials. *Journal of Analytical Atomic Spectrometry* 30, 895–902. <https://doi.org/10.1039/C4JA00328D>
- Nakada, R., Asakura, N., Nagaishi, K. (2019) Examination of analytical conditions of cerium (Ce) isotope and stable isotope ratio of Ce in geochemical standards. *Geochemical Journal* 53, 293–304. <https://doi.org/10.2343/geochemj.2.0567>
- Olivier, N., Boyet, M. (2006) Rare earth and trace elements of microbialites in Upper Jurassic coral- and sponge-microbialite reefs. *Chemical Geology* 230, 105–123. <https://doi.org/10.1016/j.chemgeo.2005.12.002>
- Plakhova, T.V., Romanchuk, A.Y., Yakunin, S.N., Dumas, T., Demir, S., Wang, S., Minasian, S.G., Shuh, D.K., Tyliczszak, T., Shiryayev, A.A., Egorov, A.V., Ianov, V.K., Kalmykov, S.N. (2016) Solubility of Nanocrystalline Cerium Dioxide: Experimental Data and Thermodynamic Modeling. *The Journal of Physical Chemistry C* 120, 22615–22626. <https://doi.org/10.1021/acs.jpcc.6b05650>
- Pourmand, A., Dauphas N., Ireland T.J. (2012) A novel extraction chromatography and MC-ICP-MS technique for rapid analysis of REE, Sc and Y: Revising CI-chondrite and Post-Archean Australian Shale (PAAS) abundances. *Chemical Geology* 291, 38–54. <https://doi.org/10.1016/j.chemgeo.2011.08.011>
- Tazoe, H., Obata, H., Gamo, T. (2007) Determination of cerium isotope ratios in geochemical samples using oxidative extraction technique with chelating resin. *Journal of Analytical Atomic Spectrometry* 22, 616–622. <https://doi.org/10.1039/b617285g>

